

Article

Higher Order Sliding Mode Control of MIMO Induction Motors: A New Adaptive Approach

Ali Karami-Mollaei¹ and Oscar Barambones^{2,*} 

¹ Faculty of Electrical and Computer Engineering, Hakim Sabzevari University, Sabzevar 9617976487, Iran; karami@hsu.ac.ir

² Department of Systems Engineering and Automatic Control, Faculty of Engineering of Vitoria-Gasteiz, University of the Basque Country UPV/EHU, Nieves Cano 12, 01006 Vitoria-Gasteiz, Spain

* Correspondence: oscar.barambones@ehu.es

Abstract: In this paper the objective is to force the outputs of nonlinear nonaffine multi-input multi-output (MIMO) systems to track those of a linear system with the desired properties. The approach is based on designing higher order sliding mode controller (HOSMC) with the definition of a new proportional-integral (PI) sliding surface. To this end, a linear state feedback with an adaptive switching gain (ASG) is applied to the nonlinear MIMO systems. Therefore, the switching gain can increase or decrease based on the system conditions. Then, the chattering is completely removed using a combination of HOSMC and ASG. Moreover, the proposed procedure is independent from the upper bound of the matched uncertainty, which is in the direction of system inputs. The finite time convergence to the sliding surface is also proved, which provides an invariance property in finite time. Note that invariance is the most important property of SMC. Finally, the general model of MIMO induction motors (IM) is used to address and to verify the proposed controller.

Keywords: higher order sliding mode control; multi-input multi-output system; chattering; adaptive control; induction motor

MSC: 93C10



Citation: Karami-Mollaei, A.; Barambones, O. Higher Order Sliding Mode Control of MIMO Induction Motors: A New Adaptive Approach. *Mathematics* **2023**, *11*, 4558. <https://doi.org/10.3390/math11214558>

Academic Editors: Mihail Ioan Abrudean and Vlad Muresan

Received: 7 October 2023

Revised: 2 November 2023

Accepted: 4 November 2023

Published: 6 November 2023



Copyright: © 2023 by the authors. Licensee MDPI, Basel, Switzerland. This article is an open access article distributed under the terms and conditions of the Creative Commons Attribution (CC BY) license (<https://creativecommons.org/licenses/by/4.0/>).

1. Introduction

In recent years and decades, much research has been conducted using a variable structure based on sliding mode control (SMC) to control nonlinear systems [1–7]. For example, SMC is used for the cart-pendulum model [2], for an electric furnace [3], for spacecraft [4], for a permanent magnet synchronous motor (PMSM) [5,6], for linear motor positioning [7], etc. This is because a traditional SMC can overcome the matched uncertainties since it is invariant, which is its most important property [8–10]. It should be noted that the robustness is weaker than the invariance [10]. Therefore, uncertainty and disturbance cannot affect the performance of SMC [10], since it is invariant [11]. However, SMC suffers from chattering phenomena, which can harm the plants [12]. Chattering is often due to the high frequency excitation of the ignored dynamics of the plants, such as sensors or actuators [9,13,14]. High frequency switching of plants' input and high controller gain are two reasons, which would excite these neglected dynamics and can produce chattering [1,15].

Generally, boundary layer SMC (BSMC), adaptive boundary layer SMC (ABSMC), dynamic SMC (DSMC), higher order SMC (HOSMC), and intelligent-based approaches are provided to remove the chattering. The invariance property is dismissed in BSMC and ABSMC, but these methods are traditionally used for SMC [8]. Nevertheless, the chattering can be reduced or suppressed using high gain inside the boundary layer [8,16]. The high gain produces instability and chattering inside the boundary [1,14].

DSMC can remove the chattering completely using an integrator. The integrator would remove high switching without using a large gain [17]. But this approach needs

an observer [17]. HOSMC can remove chattering [18], because it transfers the switching to the higher order derivatives of the sliding surface or output [9,19,20]. Some proposed approaches are based on second or higher order SMC [20,21].

Finally, intelligent-based approaches can remove the chattering, such as fuzzy systems [22,23] or neural networks. [24–27]. Most of these works focus on single-input single-output (SISO) systems or affine systems [22–27]. The intelligent-based approach can be categorized into direct and indirect structures [28]. In direct structures, intelligent methods play a direct role in the controller; but in indirect structures, intelligent methods play a secondary role in the controller [28]. However, the intelligent approaches cannot address systematic nonlinear controllers.

Note that the chattering occurs through two phenomena: high switching of input control signals and a large gain especially in a closed loop system. For example, in the literature of SMC [29,30], it is shown that the chattering can be available in super-twisting algorithms [20] or in power-fractional algorithms [31]. Both of these algorithms use a continuous input control signal with infinite gain. Then, in the concept of chattering suppression, the large gain should be considered [32]. One method to reduce the switching gain is based on an adaptive procedure, such as adaptive switching gain (ASG).

Moreover, some works in the literature focus on the control of induction motors (IM) [33,34]. But, in these works, the linearized SISO model of IM is used. The general models of IM are nonlinear, with a multi-input multi-output (MIMO) structure [35].

In this paper, HOSMC with ASG is presented to overcome these two phenomena, which can produce chattering by the excitation of unmolded dynamics of sensors or actuators. The combination of HOSMC and ASG is extended to control the general model of IM, which is MIMO and nonlinear. To this end, a linear state feedback with a new input control signal is applied to the system at first. Then, HOSMC is designed using this new input. This means that we have two types of feedback: state feedback and HOSMC feedback. In this sense, the proposed control scheme overcomes the aforementioned problems that usually appear in the traditional SMC schemes. For example, the noise on the sliding surface cannot be affected the overall system. Then, the closed loop system has an invariance property. Note that BSMC and ABSMC cannot reserve the invariance as the most important issue of a traditional SMC.

The paper is presented in six sections. In Section 2, the preliminary background of the main problem is provided. In this section, some necessary definitions and assumptions are presented. Section 3 is devoted to the HOSMC design. Definitions of the system formulation, state feedback, and sliding surface are presented in this section. The adaptive procedure and proof of the closed loop stability are presented in Section 4. In Section 5, the simulation results are presented to verify the concepts of the theory. Two simulations were conducted and are described for comparison in this section. The conclusion is available in Section 6.

2. Problem Formulation

The traditional SMC has three stages: reaching stage, sliding stage, and steady-state stage. To provide the invariance characteristic in the sliding and steady-state stages, the finite time to the sliding surface should be guaranteed. To this end, the following reaching law is used [10]:

$$\dot{s} = -\eta \operatorname{sign}(s),$$

in which, s is the sliding surface, and η is a positive large enough scalar number, which is called the switching gain. But the available Signum function produces high frequency oscillations with amplitude η in the input control signal of the systems, called chattering. The chattering is destructive and can damage the plants. Therefore, chattering should be removed by [36]:

1. Reducing the amplitude of the switching gain.
2. Eliminating high frequency switching.

The first issue is achieved using ASG, and the second issue is achieved using HOSMC. Now, consider the general model of IM in the form of a time-varying nonlinear nonaffine MIMO system as follows:

$$\begin{aligned} \dot{x} &= f(x, u, t) \\ y &= h(x, t) \end{aligned} \tag{1}$$

with the input vector signal $u = [u_1, u_2, \dots, u_m]^T \in R^{m \times 1}$, the output vector signal $y = [y_1, y_2, \dots, y_p]^T \in R^{p \times 1}$, and the state vector signal $x = [x_1, x_2, \dots, x_n]^T \in R^{n \times 1}$.

Definition 1 (Zero Dynamics). The corresponding zero dynamics of the system in Equation (1) are defined as state variables, when the outputs are set to zero.

$$\{x | y_i(x, t) = 0 : i = 1, 2, \dots, p\}$$

The system in Equation (1) is called minimum phase, if these zero dynamics are uniformly asymptotically stable [8,9].

Assumption 1. Consider the case of $p = m$. This is not a restriction assumption [14,37] (and also, see Definition 3).

Assumption 2. Output functions $y_i(x, t) : i = 1, 2, \dots, m$ are smooth, and their first $(\rho_i - 1)$ derivatives are assumed to be available either through direct measurement or via an estimator [1–9,14,19–21,38–41].

Assumption 3. We assume the relative degree of outputs $y_i : i = 1, 2, \dots, m$ with respect to the input control signals $u_i : i = 1, 2, \dots, m$; i.e., r_i is known, and the associated zero dynamics are stable [1–9,14,19–21,38–41] (see Definition 1).

Assumption 4. If $s = [s_1, s_2, \dots, s_m]^T \in R^{m \times 1}$ is a vector function, then:

$$\text{sign}(s) = [\text{sign}(s_1), \text{sign}(s_2), \dots, \text{sign}(s_m)]^T.$$

Finally, the goal is to have the outputs $y_i : i = 1, 2, \dots, m$ of the system and their first $(\rho_i - 1)$ derivatives track $y_{di} : i = 1, 2, \dots, m$ in the following desired reference linear system.

$$y_{di}(\rho_i) = f_i Y_{di} + v_{di}, \tag{2}$$

where

$$\begin{aligned} Y_{di} &= [y_{di}, y_{di}^{(1)}, \dots, y_{di}^{(\rho_i-1)}, 0, \dots, 0]^T \in R^{\rho \times 1} \\ f_i &= [f_{i1}(t), f_{i2}(t), \dots, f_{i\rho_i}(t), 0, \dots, 0] \in R^{1 \times \rho} \end{aligned}$$

Such that $\rho_i \geq r_i : i = 1, 2, \dots, m$, and

$$\rho = \max(\rho_i) : i = 1, 2, \dots, m. \tag{3}$$

Note that the system in Equation (2) can be written in the following form.

$$Y_d = \sum_{i=1}^m (\Lambda_i F Y_{di}) + V_d, \tag{4}$$

With

$$\begin{aligned} Y_d &= [y_{d1}^{(\rho_1)}, y_{d2}^{(\rho_2)}, \dots, y_{dm}^{(\rho_m)}]^T \in R^{m \times 1} \\ V_d &= [v_{d1}, v_{d2}, \dots, v_{dm}]^T \in R^{m \times 1} \\ F &= [f_1^T, f_2^T, \dots, f_m^T]^T \in R^{m \times \rho} \end{aligned}$$

and $\Lambda_i = \text{diag}(\lambda_j) \in R^{m \times m} : i, j = 1, 2, \dots, m$ is a diagonal matrix defined as follows:

$$\lambda_j = \begin{cases} 1 & j = i \\ 0 & j \neq i \end{cases}$$

Definition 2. Consider the outputs of the system in Equation (1) and let the system be closed by some possibly dynamical discontinuous feedback (such as the Signum function). Then, provided that the functions $y_i^{(j)}(x, t) : R^n \times R^+ \rightarrow R : i = 0, 1, \dots, m, j = 0, 1, \dots, \rho_i - 1$, with ρ in Equation (3), are continuous, the motion on H^ρ is called the (ρ) th order sliding mode with respect to the sliding variable $h(x, t)$ [39,40].

$$H^\rho = \left\{ x \left| \begin{array}{l} h_1(x, t) = \dot{h}_1(x, t) = \dots = h_1^{(\rho_1-1)}(x, t) = 0 \\ \vdots \\ h_m(x, t) = \dot{h}_m(x, t) = \dots = h_m^{(\rho_m-1)}(x, t) = 0 \end{array} \right. \right\}$$

Therefore, output h satisfies the following equation [41]:

$$Y_a = \phi(x, \bar{u}, t) + \gamma(x, \bar{u}, t)U_a, \tag{5}$$

where

$$\begin{aligned} Y_a &= [y_1^{(\rho_1)}, y_2^{(\rho_2)}, \dots, y_m^{(\rho_m)}]^T \in R^{m \times 1} \\ U_a &= [u_1^{(\rho_1-r_1)}, u_2^{(\rho_2-r_2)}, \dots, u_m^{(\rho_m-r_m)}]^T \in R^{m \times 1} \\ \phi &= [\phi_1, \phi_2, \dots, \phi_m]^T \in R^{m \times 1} \end{aligned}$$

$$\gamma = \begin{bmatrix} \gamma_{11} & \gamma_{12} & \dots & \gamma_{1m} \\ \gamma_{21} & \gamma_{22} & \dots & \gamma_{2m} \\ \vdots & \vdots & \ddots & \vdots \\ \gamma_{m1} & \gamma_{m2} & \dots & \gamma_{mm} \end{bmatrix} \in R^{m \times m}.$$

In $\phi_i(x, \bar{u}, t) : i = 1, 2, \dots, m$ and $\gamma_{ij}(x, \bar{u}, t) : i, j = 1, 2, \dots, m$, we have:

$$\begin{aligned} \bar{u} &= [\bar{u}_1, \bar{u}_2, \dots, \bar{u}_m]^T \\ \bar{u}_k &= [u_k, \dot{u}_k, \dots, u_k^{(\rho_i-r_i-1)}]^T : k = 1, 2, \dots, m \end{aligned}$$

The (ρ) th order sliding mode control allows the finite time convergence to the sliding surface by defining a suitable discontinuous signal $u_i^{(\rho_i-r_i)}$ [39–41].

Assumption 5. Suppose ϕ and γ are unknown bounded functions probably with known bounds [19,20,38,40,41].

Assumption 6. Suppose $\gamma_{ii} \neq 0 : \forall t \geq 0, i = 1, 2, \dots, m$. This assumption is not restrictive [19,20,38,40,41].

Definition 3. The differential system in Equation (1) is called proper if [37]:

- $p = m$; i.e., the input and output dimensions are equal,
- All $\phi_i : i = 1, 2, \dots, m$ are C^1 functions,
- All $\gamma_{ij} : i, j = 1, 2, \dots, m$ are C^1 functions,
- $\gamma_{ii} \neq 0 : \forall t \geq 0, i = 1, 2, \dots, m$.

3. Controller Design

Defining

$$\begin{aligned}
 e_i &= y_i - y_{di} : i = 1, 2, \dots, m \\
 E_a &= [e_1(\rho_1 - 1), e_2(\rho_2 - 1), \dots, e_m(\rho_m - 1)] - T \in R^{m \times 1} \\
 E_i &= [e_i, e_i(1), \dots, e_i(\rho_i - 1), 0, \dots, 0] - T \in R^{\rho_i \times 1} \\
 Y_i &= [y_i, y_i(1), \dots, y_i(\rho_i - 1), 0, \dots, 0] - T \in R^{\rho_i \times 1},
 \end{aligned}$$

We have:

$$\begin{aligned}
 \dot{E}_a &= Y_a - Y_d = \phi + \gamma U_a - \sum_{i=1}^m (\Lambda_i F Y_{di}) - V_d = \\
 \phi + \gamma U_a - \sum_{i=1}^m (\Lambda_i F Y_{di}) - V_d + \sum_{i=1}^m (\Lambda_i F Y_i) - \sum_{i=1}^m (\Lambda_i F Y_i) + V_r - V_r + U_a - U_a &= \quad (6) \\
 \sum_{i=1}^m (\Lambda_i F E_i) + V_r - V_d + (\phi + \gamma U_a - U_a) + (U_a - \sum_{i=1}^m (\Lambda_i F Y_i) - V_r)
 \end{aligned}$$

Now, we apply the following linear state feedback with $V_r \in R^{m \times 1}$ as the new input control signal to Equation (6):

$$U_a = \sum_{i=1}^m (\Lambda_i F Y_i) + V_r, \quad (7)$$

with the matched uncertainty variable as

$$W = (\phi + \gamma U_a - U_a).$$

We conclude that

$$\dot{E}_a = \sum_{i=1}^m (\Lambda_i F E_i) + V_r - V_d + W. \quad (8)$$

Note that the matched uncertainties are in the inputs' directions and can be cancelled out directly by the input control signals of the plant [42].

The greatest challenge of SMC is providing a suitable input control signal $V_r(t)$ in Equation (7), such that the states of system Equation (5), Y_a , track the states of system Equation (4), Y_d ; in other words, the error dynamic in Equation (8) converges to zero in finite time, even in the presence of the matched uncertainties. Therefore, we define the following PI sliding surface.

$$s(t) = \sigma E_a(t) - \int_0^t \left(\sum_{i=1}^m (\Lambda_i [\sigma F(\tau) + K(\tau)] E_i(\tau)) + \zeta(\tau) \right) d\tau, \quad (9)$$

in which

$$\begin{aligned}
 s &= [s_1, s_2, \dots, s_m]^T \in R^{m \times 1} \\
 \zeta &= [\zeta_1, \zeta_2, \dots, \zeta_m]^T \in R^{m \times 1} \\
 K &= \begin{bmatrix} k_{11} & k_{12} & \dots & k_{1\rho_1} & 0 & \dots & 0 \\ k_{21} & k_{22} & \dots & k_{2\rho_2} & 0 & \dots & 0 \\ \vdots & \vdots & \vdots & \vdots & \vdots & \ddots & \vdots \\ k_{m1} & k_{m2} & \dots & k_{m\rho_m} & 0 & \dots & 0 \end{bmatrix} \in R^{m \times \rho},
 \end{aligned}$$

Whenever $K(t)$, $\zeta(t)$ and $\sigma \in R^{m \times m}$ are design parameters. The derivative of the sliding surface Equation (9) with respect to time leads to:

$$\dot{s}(t) = \sigma \dot{E}_a(t) - \sum_{i=1}^m (\Lambda_i [\sigma F(t) + K(t)] E_i) - \zeta(t). \quad (10)$$

The matrix σ can be chosen such that the interferences between the input and output in different channels of the MIMO system are removed. In this case, the MIMO system is decoupled to several SISO systems with specific input and output directions, leading to a simpler design. Then, we have chosen $\sigma = I_{m \times m}$, in which I is the identity matrix. Now, by substitution of Equation (8) into Equation (10) one obtains:

$$\dot{s}(t) = (V_r - V_d + W) - \sum_{i=1}^m (\Lambda_i K(t) E_i) - \zeta(t).$$

The control input $V_r(t)$ has two parts in the sliding stage and the steady-state stage, a smooth equivalent part when $\dot{s} = 0$ and $W = 0$ and a discontinuous part when $\dot{s} = -\eta \text{sign}(s)$ to overcome the matched uncertainty $W \neq 0$ [8–10].

Therefore, the equivalent section V_{req} is obtained as follows.

$$V_{req} = (V_d + \zeta(t)) + \sum_{i=1}^m (\Lambda_i K(t) E_i)$$

In this case, the dynamic of error is obtained by substituting V_{req} into Equation (8) and setting $W = 0$.

$$\dot{E}_a(t) = \sum_{i=1}^m (\Lambda_i (F + K) E_i) + \zeta \tag{11}$$

Linear Equation (11) yields the zero dynamics of the sliding surface, which should be stabilized by the proper choosing of matrix $K(t)$ and vector signal $\zeta(t)$ (refer to Assumption 3).

At first, we suppose that $\zeta(t) = 0$, and we choose

$$K(t) = M - F(t), \tag{12}$$

where

$$M = \begin{bmatrix} m_{11} & m_{12} & \dots & m_{1\rho_1} & 0 & \dots & 0 \\ m_{21} & m_{22} & \dots & m_{2\rho_2} & 0 & \dots & 0 \\ \vdots & \vdots & \ddots & \vdots & \vdots & \ddots & \vdots \\ m_{m1} & m_{m2} & \dots & m_{m\rho_m} & 0 & \dots & 0 \end{bmatrix} \in R^{m \times \rho}.$$

Then the following Linear-Time-Invariant (LTI) system is obtained and should be stabilized by the proper choice of the constants m_{ij} .

$$\dot{E}_a = \sum_{i=1}^m (\Lambda_i M E_i)$$

Now, consider the case $\zeta(t) \neq 0$ in equation (11). It can be calculated to have terminal SMC [4–6,31,43,44] i.e., the error signal converges to zero in finite time. We consider t_f as the time reaching to the sliding surface. Suppose the system is on the sliding surface Equation (9), which means that $t \geq t_f$. Then, the error trajectories converge to zero in finite time $t_e + t_f$ with

$$t_e \leq \frac{\|E_a(0)\|}{\eta_e}. \tag{13}$$

To this end, we choose:

$$\zeta(t) = -\eta_e \text{sign} \left(E_a(t) - \int_0^t \sum_{i=1}^m (\Lambda_i M E_i(\tau)) d\tau \right),$$

with $\eta_e > 0$, and we define $s_e \in R^{m \times 1}$ as follows:

$$s_e = E_a(t) - \int_0^t \sum_{i=1}^m (\Lambda_i M E_i(\tau)) d\tau.$$

Using Equations (11) and (12) yields

$$\dot{s}_e = \zeta = -\eta_e \text{sign}(s_e).$$

The Lyapunov function candidate as $V(t) = 0.5s_e^T s_e$ results in

$$\dot{V} = s_e \dot{s}_e = -\eta_e s_e \text{sign}(s_e),$$

Which is Negative-Definite (ND); therefore,

$$s_{ei} \dot{s}_{ei} = -\eta_e s_{ei} \text{sign}(s_{ei}) = -\eta_e |s_{ei}| : i = 1, 2, \dots, m.$$

Integration of this equation leads to (see proof of Theorem 2):

$$t_{ei} = \frac{|s_{ei}(0)|}{\eta_e} \leq \frac{\|s_e(0)\|}{\eta_e} = \frac{\|E_a(0)\|}{\eta_e} : i = 1, 2, \dots, m.$$

This leads to Equation (13), where $t_e = \max(t_{ei}) : i = 1, 2, \dots, m$.

The second part of the input variable, $V_r(t)$, is discontinuous and the force moving the states of the system toward the sliding surface in finite time even in the presence of a matched uncertain W . This causes the closed loop system to be invariant. Therefore, the following adaptive input control signal is proposed, which consists of an equivalent control part plus a discontinuous control part.

$$V_r(t) = \sum_{i=1}^m (\Lambda_i K(t) E_i) + V_d + \zeta(t) - \eta \text{sign}(s), \tag{14}$$

where $\eta = (p_1 + 1)\beta$ is the switching gain, $p_1 > 0$ is a constant, and $\beta(t) > 0 : \forall t$ is an adaptive parameter.

Assumption 7 (Upper Bound of Matched Uncertainty). *We assume that $W(x, \bar{u}, U_a, t)$ is norm-bounded by a probably known function $\Omega(x, \bar{u}, U_a, t)$, which means that $\|W(x, \bar{u}, U_a, t)\| \leq \Omega(x, \bar{u}, U_a, t) < \infty$. Generally, this inequality is popular and is not restrictive [1,8,9,20,39,41]. Moreover, with respect to other available uncertainty handling approaches [8,9,14,19–21,38–41], we need the matched uncertain W to be norm-bounded, but the magnitude of this bound Ω can be unknown (see Remark 1).*

4. Adaptive Approach

A simple adaptive method of $\beta(t)$ is as follows:

$$\begin{aligned} \dot{\beta} &= \dot{\Omega} + p_2 \|s\|, \beta(0) = \beta_0, \Omega(0) = \Omega_0, \\ \Omega_0 &= \Omega(x(0), \bar{u}(0), U_a(0), 0) \end{aligned} \tag{15}$$

where $p_2 > 0$ is a constant parameter, and Ω_0 and arbitrary β_0 are the bounded initial values of Ω and β , respectively. Equation (15) has practical important drawbacks. Parameter β is increasing. For example, the available noise or chattering on the sliding surface or a large initial distance from the sliding surface causes the parameters β and switching gain η to increase quickly, which results in closed loop instability. Moreover, when the system conditions change such that a smaller switching gain is permitted, the law of Equation (15) cannot adapt itself to these new circumstances.

Therefore, to overcome these practical challenges, the adaptive parameter β is modified as follows, which can be increased and decreased based on the circumstances.

$$\begin{aligned} \dot{\beta} &= \dot{\Omega} + p_2(\|s\| - \psi(\beta)), \beta(0) = \beta_0, \Omega(0) = \Omega_0 \\ \psi(\beta) &= \frac{\varepsilon_1}{2}(\text{sign}(\beta - \Omega - \varepsilon_0) + 1) \geq 0 \end{aligned} \tag{16}$$

Due to the available negative feedback in this equation, the instability will not occur. Constants $p_2 > 0$, $\varepsilon_1 > 0$, and $\varepsilon_0 > 0$ are design parameters, and Ω_0 and arbitrary β_0 are the bounded initial values of Ω and β , respectively. Integrating the first part of Equation (16), we conclude:

$$\beta(t) = \Omega(t) + \beta_0 - \Omega_0 + p_2 \int_0^t (\|s(\tau)\| - \psi) d\tau. \tag{17}$$

Lemma 1. *The following inequality:*

$$\mu(0) = \mu_0 = \beta_0 - \Omega_0 > \varepsilon_0 > 0, \tag{18}$$

together with Equation (16) results in:

$$\mu(t) = \beta - \Omega \geq \varepsilon_0 : \forall t > 0.$$

Proof. Equations (16) and (17) lead to

$$\mu(t) = \mu_0 + p_2 \int_0^t \|s(\tau)\| d\tau - \frac{p_2 \varepsilon_1}{2} \int_0^t (\text{sign}(\mu - \varepsilon_0) + 1) d\tau.$$

It is clear that $\mu(t)$ is continuous function and also $\mu_0 > \varepsilon_0$. Then, there is a finite time t_1 , such that:

$$\begin{aligned} \mu(t) &> \varepsilon_0 : \forall t \in [0, t_1) \\ t_1 &\geq \frac{2(\mu_0 - \varepsilon_0)}{p_2 \varepsilon_1} \end{aligned} .$$

Therefore, at time $t = t_1$, we have $\mu(t_1) = \varepsilon_0$; i.e.,

$$\varepsilon_0 = \mu_0 + p_2 \int_0^{t_1} \|s(\tau)\| d\tau - \frac{p_2 \varepsilon_1 t_1}{2}.$$

Now, suppose that there is a time t_2 such that,

$$\mu(t) < \varepsilon_0 : \forall t \in (t_1, t_2). \tag{19}$$

Then, the equation:

$$\mu(t) = \mu_0 + p_2 \int_0^{t_1} \|s(\tau)\| d\tau + p_2 \int_{t_1}^t \|s(\tau)\| d\tau - \frac{p_2 \varepsilon_1 t_1}{2}$$

results in the following equality.

$$\mu(t) = \varepsilon_0 + p_2 \int_{t_1}^t \|s(\tau)\| d\tau$$

The righthand side is always positive; therefore,

$$\mu(t) \geq \varepsilon_0 : \forall t \in (t_1, t_2).$$

This contradicts Equation (19); i.e., $\mu(t) \geq \varepsilon_0 : \forall t$. \square

Theorem 1. *Input control Equation (14) and adaptive procedure Equation (16) cause error dynamic Equation (8) to converge to sliding surface Equation (9), when the inequality in Equation (18) is fulfilled.*

Proof. Using the Lyapunov candidate function as follows:

$$V(t) = \frac{1}{2} \left(s^T s + p_2^{-1} \mu^2 \right), \tag{20}$$

one can write

$$\dot{V} = s^T \dot{s} + p_2^{-1} \mu \dot{\mu} = s^T (V_r - V_d + W - \sum_{i=1}^m (\Lambda_i K E_i) - \zeta) + p_2^{-1} \mu (\dot{\beta} - \dot{\Omega}).$$

Equations (14) and (16) result in

$$\begin{aligned} \dot{V} &= s^T (W - (p_1 + 1)\beta \operatorname{sign}(s)) + p_2^{-1} (\beta - \Omega) p_2 (\|s\| - \psi) \\ &\leq \Omega \|s\| - (p_1 + 1)\beta \|s\| + (\beta - \Omega) (\|s\| - \psi) = -p_1 \beta \|s\| - \psi \mu. \end{aligned} \tag{21}$$

Using lemma 1 leads to $\dot{V} \leq -p_1 \beta \|s\|$. By definition of the variable $\omega(t) = p_1 \beta \|s(t)\|$, one can write $\dot{V} \leq -\omega(t) \leq 0$. The integration of this inequality is concluded to be

$$0 \leq \int_0^t \omega(\tau) d\tau \leq \int_0^t \omega(\tau) d\tau + V(t) \leq V(0).$$

Note that $V(0)$ is positive and finite; then, based on Barbalat’s lemma [8,45], we obtain the following equality even in the case of $t \rightarrow \infty$.

$$\lim_{t \rightarrow \infty} \omega(t) = \lim_{t \rightarrow \infty} p_1 \beta \|s(t)\| = 0$$

Since $p_1 > 0$ and $\beta > 0$, then $\lim_{t \rightarrow \infty} \|s\| = 0$ or $\lim_{t \rightarrow \infty} s = 0$. Now, the proof of the theorem is complete. \square

In SMC, convergence to the sliding surface should happen in finite time to preserve the invariance property. The next theorem proves the finite time convergence to the sliding surface.

Theorem 2. *The error trajectory converges to the sliding surface Equation (9) in finite time t_f , when Equation (18) is provided.*

$$t_f \leq \frac{\|E_a(0)\|}{\varepsilon_0} \tag{22}$$

Proof. From Equations (20) and (16), one can write:

$$\dot{V} = s^T \dot{s} + p_2^{-1} \mu (\dot{\beta} - \dot{\Omega}) = s^T \dot{s} + p_2^{-1} \mu p_2 (\|s\| - \psi) = s^T \dot{s} + \mu \|s\| - \mu \psi.$$

Using Equation (21),

$$\dot{V} = s^T \dot{s} + \mu \|s\| - \mu \psi \leq -p_1 \beta \|s\| - \psi \mu.$$

Thus,

$$s^T \dot{s} + \mu \|s\| \leq -p_1 \beta \|s\|.$$

Since $p_1 > 0, \beta > 0$ and $\|s\| \geq 0$, we have $s^T \dot{s} + \mu \|s\| \leq 0$ or $s^T \dot{s} \leq -\mu \|s\|$. From Lemma 1, we can write $-\mu \leq -\varepsilon_0$; therefore,

$$s^T \dot{s} \leq -\varepsilon_0 \|s\| = -\varepsilon_0 (s^T s)^{\frac{1}{2}}.$$

Then, $s_i \dot{s}_i \leq -\varepsilon_0 (s_i s_i)^{\frac{1}{2}} = -\varepsilon_0 s_i : i = 1, 2, \dots, m$, where $\varepsilon_0 > 0$. Suppose t_{fi} is the reaching time to the sliding surface s_i ; i.e., $s_i(t_{fi}) = 0$. Now, consider two cases: First case: if $s_i > 0$, then $\dot{s}_i \leq -\varepsilon_0$, and integrating this equation between $t = 0$ and $t = t_{fi}$ leads to $-s_i(0) \leq -\varepsilon_0 t_{fi}$; therefore,

$$t_{fi} \leq \frac{s_i(0)}{\varepsilon_0}.$$

Second case: if $s_i < 0$, then $\dot{s}_i \geq \varepsilon_0$, and integrating this equation between $t = 0$ and $t = t_{fi}$ leads to $-s_i(0) \geq \varepsilon_0 t_{fi}$; therefore,

$$t_{fi} \leq \frac{-s_i(0)}{\varepsilon_0}.$$

Combining these two last equations results in

$$t_{fi} \leq \frac{|s_i(0)|}{\varepsilon_0} \leq \frac{\|s(0)\|}{\varepsilon_0} : i = 1, 2, \dots, m,$$

which lead to Equation (22), where $t_f = \max(t_{fi}) : i = 1, 2, \dots, m$. \square

Remark 1. If Ω is set to a large positive constant, then $\dot{\Omega} = 0$; in this case, Ω is only used to prove the theorems, the controller and adaptive procedure are independent of the uncertainty bound, and we have

$$\begin{aligned} \dot{\beta} &= p_2(\|s\| - \psi(\beta)), \beta(0) = \beta_0, \Omega(0) = \Omega_0 \\ \psi(\beta) &= \frac{\varepsilon_1}{2}(\text{sign}(\beta - \varepsilon_0) + 1) \geq 0 \\ \beta_0 > \varepsilon_0 > 0 &\Rightarrow \beta(t) > \varepsilon_0 > 0 : \forall t \end{aligned} \tag{23}$$

Remark 2. In the proposed method, the singular case, as discussed in [6,26], will not occur.

5. Simulation Results

The overall dynamics of an IM in stationary reference framework under the assumptions of equal mutual inductances and linear magnetic circuits are given by the following general equations [35].

$$\begin{bmatrix} \dot{x}_1 \\ \dot{x}_2 \\ \dot{x}_3 \\ \dot{x}_4 \\ \dot{x}_5 \end{bmatrix} = \begin{bmatrix} \lambda(x_2 x_5 - x_3 x_4) - \frac{T_l}{J} \\ -ax_2 - n_p x_1 x_3 + aMx_4 \\ -ax_3 + n_p x_1 x_2 + aMx_5 \\ abx_2 + n_p b x_1 x_3 - \gamma x_4 \\ abx_3 - n_p b x_1 x_2 - \gamma x_5 \end{bmatrix} + \begin{bmatrix} 0 & 0 \\ 0 & 0 \\ 0 & 0 \\ \frac{1}{\sigma} & 0 \\ 0 & \frac{1}{\sigma} \end{bmatrix} \begin{bmatrix} u_1 \\ u_2 \end{bmatrix}, \tag{24}$$

where $x = [x_1, x_2, x_3, x_4, x_5]^T = [\omega, \psi_a, \psi_b, i_a, i_b]^T$ and

$$\begin{aligned} \lambda &= \frac{n_p M}{J L_r}, a = \frac{R_r}{L_r}, b = \frac{M}{\sigma L_r}, \\ \sigma &= L_s - \frac{M^2}{L_r}, \gamma = \frac{M^2 R_r}{\sigma L_r^2} + \frac{R_s}{\sigma} \end{aligned}$$

The IM motor parameters values are set as $R_s = 0.1 \Omega, R_r = 0.15 \Omega, L_s = 0.0699 H, L_r = 0.0699 H, M = 0.068 H, J = 0.0586 \text{ kg m}^2, n_p = 1$, and $T_l = 70 \text{ Nm}$. Moreover, R_s and R_r are the stator and rotor resistances, respectively, and L_s and L_r are the stator and rotor inductances, respectively, M is the mutual inductance, J is the rotor inertia, n_p is the

number of pole pairs, ω is the rotor speed, ψ_a and ψ_b are the rotor flux components, i_a and i_b are the stator current components, and finally, T_l is the load torque. These parameters are used in the simulation of system itself not in the controller, since Ω is supposed to be constant; i.e., the controller is model free. The outputs to be controlled are the motor speed ω and the square of the rotor flux magnitude, i.e., $(\psi_a^2 + \psi_b^2)$, with the relative degrees $r_1 = r_2 = 2$ as follows:

$$\begin{bmatrix} y_1 \\ y_2 \end{bmatrix} = \begin{bmatrix} x_1 \\ x_2^2 + x_3^2 \end{bmatrix}.$$

To remove the switching of the input control signal, we choose $\rho_1 = \rho_2 = 3$ [39], and then the third-order SMC i.e., $\rho = 3$ is applied to the system. Therefore,

$$\begin{bmatrix} y_1^{(3)} \\ y_2^{(3)} \end{bmatrix} = \begin{bmatrix} \phi_1(x) \\ \phi_2(x) \end{bmatrix} + \begin{bmatrix} \gamma_{11}(x) & \gamma_{12}(x) \\ \gamma_{21}(x) & \gamma_{22}(x) \end{bmatrix} \begin{bmatrix} \dot{u}_1 \\ \dot{u}_2 \end{bmatrix}. \tag{25}$$

We want the states of system Equation (25), i.e., $y_i^{(j)} : i = 1, 2, j = 0, 1, 2$, to track the states of the linear system $y_{di}^{(3)} = f_i Y_{di} + v_{di} : i = 1, 2$; i.e., $Y_{di} = [y_{di}, y_{di}^{(1)}, y_{di}^{(2)}]^T : i = 1, 2$.

$$F = \begin{bmatrix} -3 & -5 & -3 \\ 0 & 0 & 0 \end{bmatrix},$$

and

$$\begin{matrix} v_{d1} = \sin(0.5t), \zeta_1 = 0 \\ v_{d2} = 0, \zeta_2 = 0 \end{matrix}.$$

This means that when the motor speed varies, the rotor flux is maintained constant at 0.7 Weber. Then, we choose

$$K = \begin{bmatrix} 0 & 0 & 0 \\ -3 & -5 & -3 \end{bmatrix}.$$

Other parameters are chosen as $p_1 = 1.08, p_2 = 0.05, \varepsilon_0 = 0.01, \varepsilon_1 = 1.2$. All the initial values of the system states are assumed to be set randomly. The simulations were conducted on a PC computer with an Intel(R) Pentium(R) two cores CPU with G4400@3.30GHz and a 3.30 GHz processor, with 16 GB of memory, running MATLAB version 2022. In order to carry out the simulations, a sample time of 0.01 was used. The procedure and algorithm for calculating the input control signal $u = [u_1, u_2, \dots, u_m]^T \in R^{m \times 1}$ is as follows:

1. Calculate K and ζ (or one can set $\zeta = 0$).
2. Calculate E_a and also E_i .
3. Calculate the sliding surface using Equation (9).
4. Calculate the switching gain β using Equation (23).
5. Calculate V_r via Equation (14).
6. Calculate U_a based on the previous parameters.
7. Calculate the elements of input vector u by numerical integration.

Example 1. The simulation results are shown in Figures 1–4 for two channels of input–output. Figure 1 shows the good tracking of the first output and its derivatives. From Figure 2, we can see that the switching gain increases at first to force the sliding surface toward zero in the presence of uncertainty. In this case, chattering is seen in the input control signal of the state feedback and the input control signal of the system. After that, the switching gain decreases, and the chattering is removed from all closed loop signals such as the sliding surface, input signal of state feedback, and input control of the system. Note that chattering-free of input control signal is very important, since it is applied to the plant directly. The same good tracking and chattering-less in the input control signal of the plant is also shown in Figures 3 and 4.

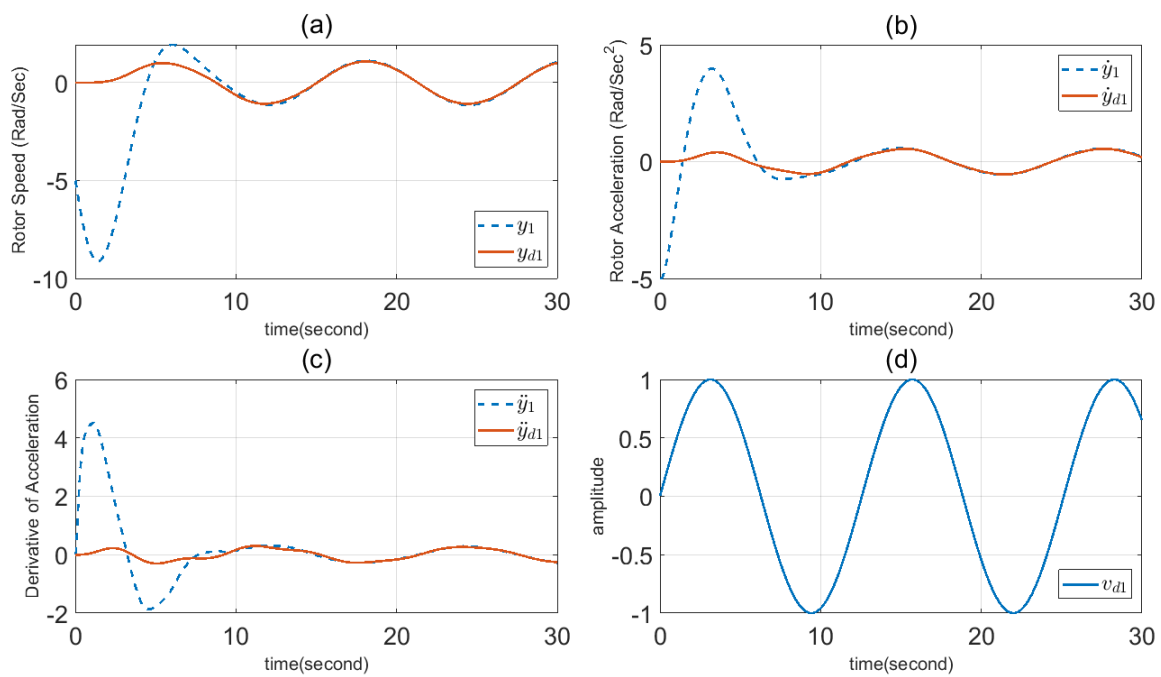


Figure 1. Reference signal tracking, (a) system output, (b) first derivative of system output, (c) second derivative of system output, and (d) input control signal of reference system in the first channel (in Example 1).

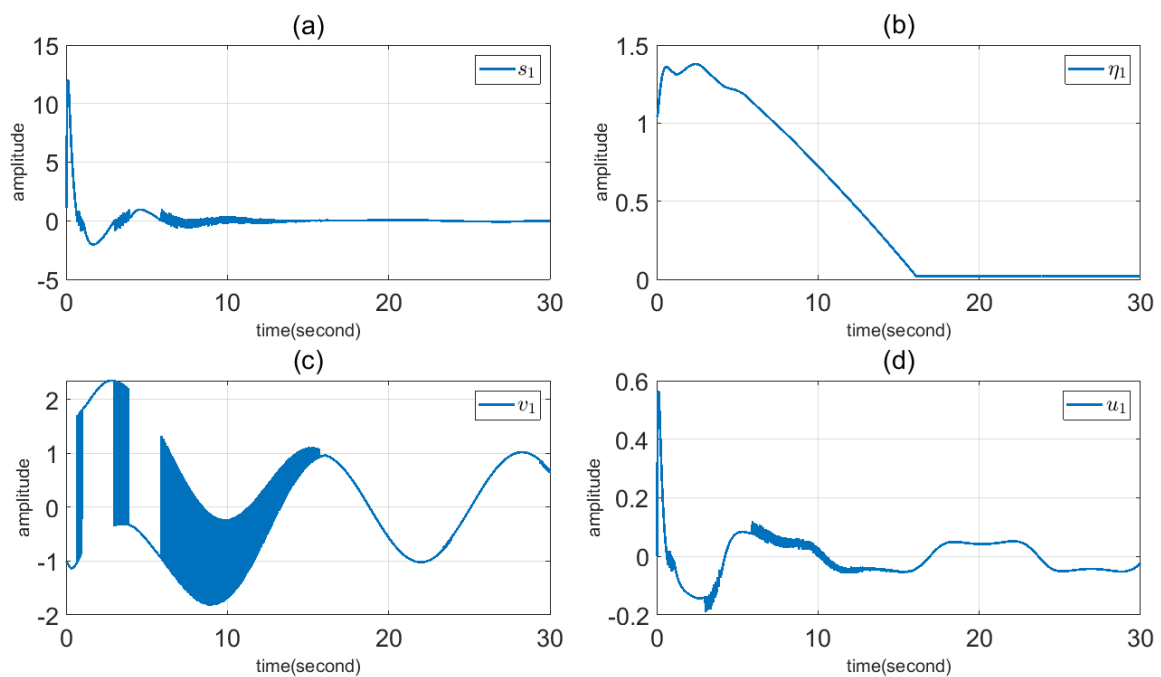


Figure 2. (a) Sliding surface, (b) switching gain, (c) input control signal of state feedback, and (d) first input control in the first channel (in Example 1).

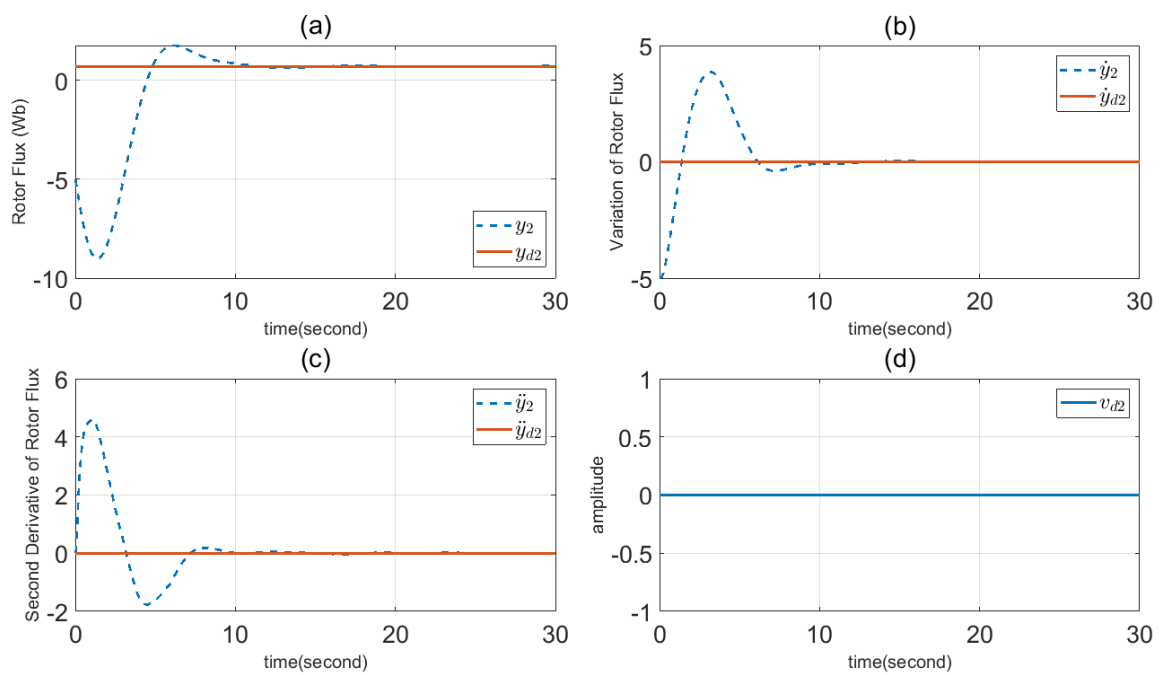


Figure 3. Reference signal tracking, (a) system output, (b) first derivative of system output, (c) second derivative of system output, and the (d) input control signal of reference system in the second channel (in Example 1).

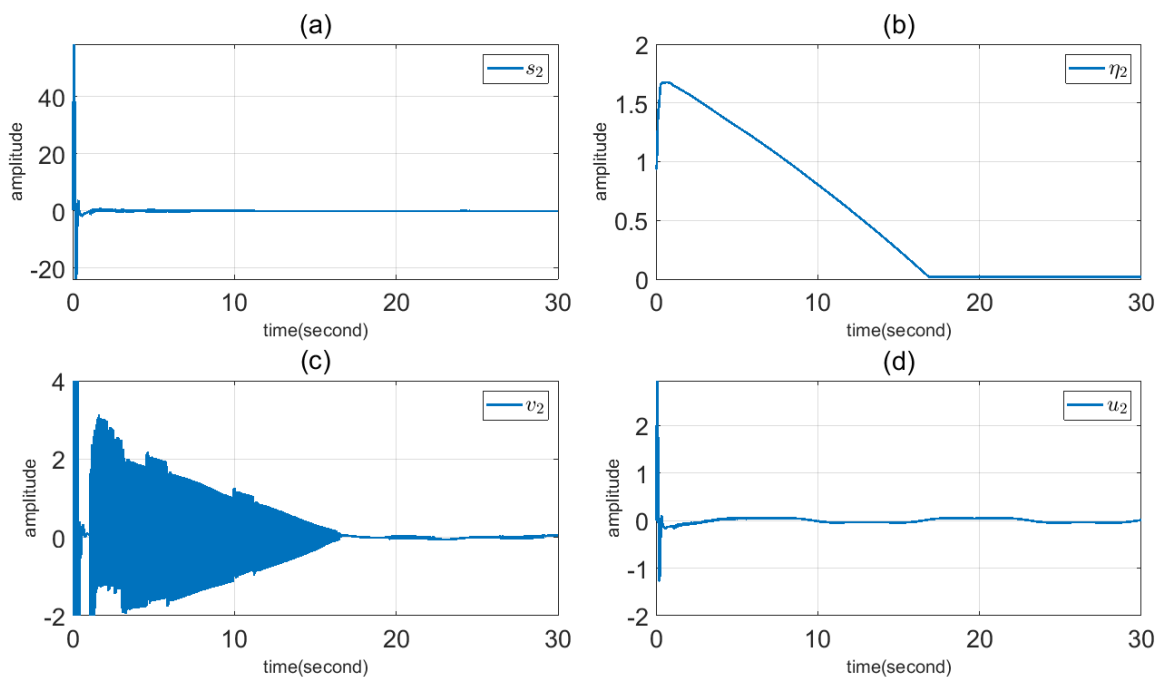


Figure 4. (a) Sliding surface, (b) switching gain, (c) input control signal of state feedback, and the (d) second input control signal of system in the second channel (in Example 1).

Example 2. All the parameters are chosen as in the previous example except the $\psi(\beta)$, which is set to zero; i.e., $\psi(\beta) = 0$. Only the sliding surface, switching gain, input control of state feedback, and input control signal of the system are shown in the two channels. The drift and increase in the switching gain are shown in Figures 5 and 6. This can cause instability of the closed loop system.

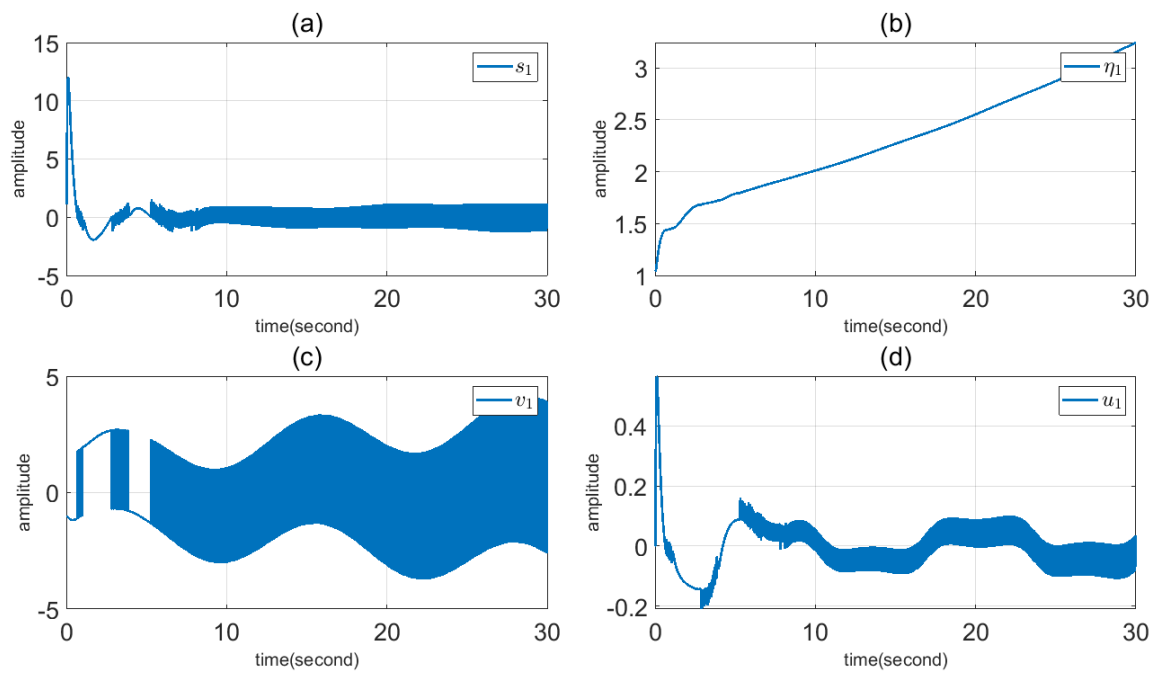


Figure 5. (a) Sliding surface, (b) switching gain, (c) input control signal of state feedback, and the (d) second input control signal of the system in the first channel (in Example 2).

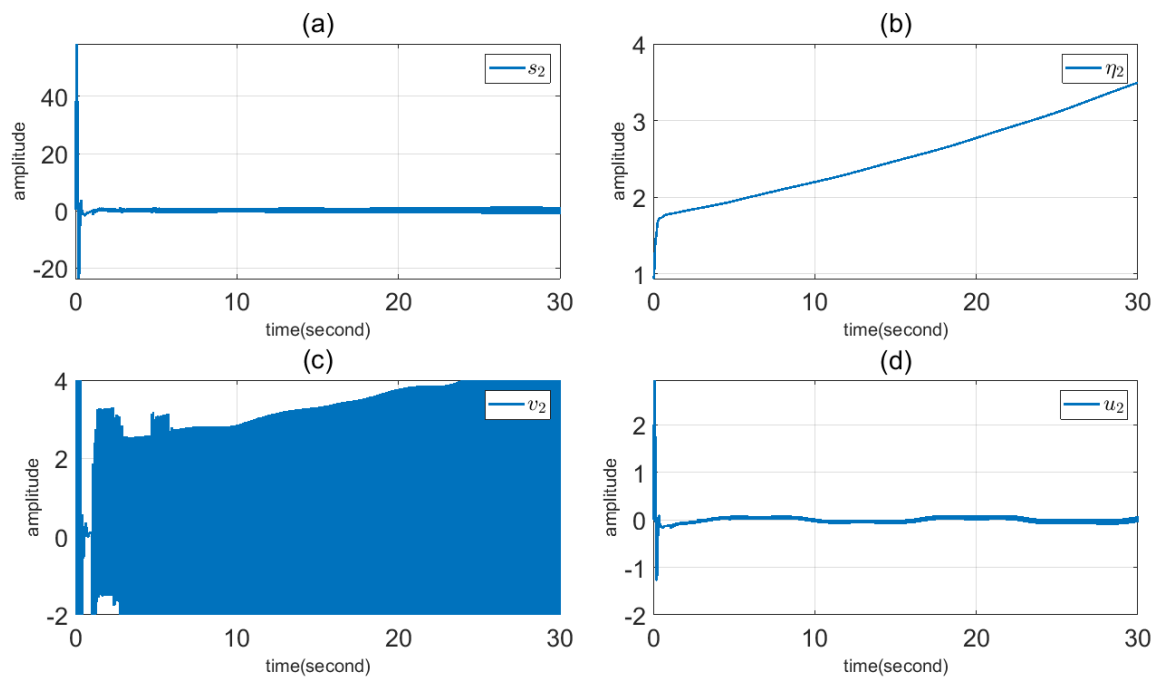


Figure 6. (a) Sliding surface, (b) switching gain, (c) input control signal of state feedback, and the (d) second input control signal of the system in the second channel (in Example 2).

From the figures presented in Examples 1 and 2, one can see the advantages of the proposed approach in chattering suppression over traditional SMC schemes. Moreover, due to negative feedback, the drift and instability can be avoided.

6. Conclusions

A new method of higher order sliding mode control (HOSMC) for nonlinear multi-input multi-output (MIMO) systems is proposed. Linear state feedback was used at first,

and then sliding mode control (SMC) was designed. After that, an adaptive procedure was constructed, which can increase and decrease the switching gain based on the system conditions. Therefore, using a combination of the HOSMC and adaptive switching gain (ASG), the performance of the closed loop system in chattering suppression was improved. To preserve the invariance property, as the most important characteristic of the SMC, finite time convergence to the proportional-integral (PI) sliding surface was proved. Finally, in the proposed approach, the upper bound of the uncertainty does not need to be available. The proposed method is applied to the control of MIMO induction motors (IM). The simulation results showed the effectiveness of this method. The proposed method also preserves all the main properties of SMC, such as invariance and simplicity of a systematic implementation. Future work can be based on designing fractional HOSMC for MIMO systems.

Author Contributions: Conceptualization, methodology, and writing: A.K.-M.; original draft preparation, validation, review, and editing: O.B. All authors have read and agreed to the published version of the manuscript.

Funding: This research received no external funding.

Data Availability Statement: There is no data availability.

Acknowledgments: The authors wish to express their gratitude to the Basque Government, through the project EKOHEGAZ II (ELKARTEK KK-2023/00051), to the Diputación Foral de Álava (DFA), through the project CONAVANTER, to the UPV/EHU, through the project GIU20/063, and to the MobilityLab Foundation (CONV23/14. Proy. 16) for supporting this work.

Conflicts of Interest: The authors declare no conflict of interest.

References

1. Young, K.D.; Utkin, V.I.; Ozguner, U. A control engineer's guide to sliding mode control. *IEEE Trans. Control Syst. Technol.* **1999**, *7*, 328–342. [[CrossRef](#)]
2. Li, Y.; Zhang, H.; Xie, X.; Xia, J. Stability analysis of a cart-pendulum model with variable convergence rate: A sliding mode control approach for impulsive stochastic systems. *Chaos Solitons Fractals* **2023**, *175*, 114044. [[CrossRef](#)]
3. Rsetam, K.; Al-Rawi, M.; Cao, Z. Robust adaptive active disturbance rejection control of an electric furnace using additional continuous sliding mode component. *ISA Trans.* **2022**, *130*, 152–162. [[CrossRef](#)] [[PubMed](#)]
4. Liu, K.; Wang, Y.; Ji, H.; Wang, S. Adaptive saturated tracking control for spacecraft proximity operations via integral terminal sliding mode technique. *Int. J. Robust Nonlinear Control* **2021**, *31*, 9372–9396. [[CrossRef](#)]
5. Zhao, K.; Liu, W.; Zhou, R.; Dai, W.; Wu, S.; Qiu, P.; Yin, Y.; Jia, N.; Yi, J.; Huang, G. Model-free fast integral terminal sliding-mode control method based on improved fast terminal sliding-mode observer for PMSM with unknown disturbances. *ISA Trans.* **2023**, *in press*. [[CrossRef](#)]
6. Zhang, L.; Tao, R.; Zhang, Z.-X.; Chien, Y.-R.; Bai, J. PMSM non-singular fast terminal sliding mode control with disturbance compensation. *Inf. Sci.* **2023**, *642*, 119040. [[CrossRef](#)]
7. Shao, K.; Zheng, J.; Huang, K.; Wang, H.; Man, Z.; Fu, M. Finite-time control of a linear motor positioner using adaptive recursive terminal sliding mode. *IEEE Trans. Ind. Electron.* **2020**, *67*, 6659–6668. [[CrossRef](#)]
8. Slotine, J.-J.E.; Li, W. *Applied Nonlinear Control*; Prentice-Hall: Hoboken, NJ, USA, 1991.
9. Perruquetti, W.; Pierre-Barbot, J. *Sliding Mode Control in Engineering*; Marcel Dekker: New York, NY, USA, 2002.
10. Gao, W.; Hung, J.C. Variable structure control of nonlinear systems: A new approach. *IEEE Trans. Ind. Electron.* **1993**, *40*, 45–55.
11. Hansen, A.; Li, Y.; Hedrick, J.K. Invariant sliding domains for constrained linear receding horizon tracking control. *IFAC J. Syst. Cont.* **2017**, *2*, 12–17. [[CrossRef](#)]
12. Su, J.-P.; Wang, C.-C. Complementary sliding control of non-linear systems. *Inter. J. Cont.* **2002**, *75*, 360–368. [[CrossRef](#)]
13. Bartolini, G.; Pydynowski, P. An improved, chattering free, V.S.C. scheme for uncertain dynamical systems. *IEEE Trans. Automat. Contr.* **1996**, *41*, 1220–1226. [[CrossRef](#)]
14. Bartolini, G.; Ferrara, A.; Usai, E.; Utkin, V.I. On multi-input chattering-free second-order sliding mode control. *IEEE Trans. Automat. Contr.* **2000**, *45*, 1711–1717. [[CrossRef](#)]
15. Boiko, I.; Fridman, L.; Pisano, A.; Usai, E. Analysis of chattering in systems with second-order sliding modes. *IEEE Trans. Automat. Contr.* **2007**, *52*, 2085–2102. [[CrossRef](#)]
16. Chen, M.-S.; Hwang, Y.-R.; Tomizuka, M. A state-dependent boundary layer design for sliding mode control. *IEEE Trans. Automat. Contr.* **2002**, *47*, 1677–1681. [[CrossRef](#)]
17. Karami-Mollae, A.; Shojaei, A.A.; Barambones, O.; Fauzi Othman, M. Dynamic sliding mode control of pitch blade wind turbine using sliding mode observer. *Trans. Inst. Meas. Control* **2022**, *44*, 3028–3038. [[CrossRef](#)]

18. Emelyanov, S.V.; Korovin, S.K.; Levant, A. Higher-order sliding modes in control systems. *Comput. Math. Modeling*. **1996**, *7*, 294–318. [[CrossRef](#)]
19. Barambones, O.; Cortajarena, J.A.; Calvo, I.; Conzales de Durana, J.M.; Alcorta, P.; Karami-Mollae, A. Real time observer and control scheme for a wind turbine system based on a high order sliding modes. *J. Franklin Inst.* **2021**, *358*, 5795–5819. [[CrossRef](#)]
20. Levant, A. Sliding order and sliding accuracy in sliding mode control. *Inter. J. Contr.* **1993**, *58*, 1247–1263. [[CrossRef](#)]
21. Bartolini, G.; Ferrara, A.; Usai, E. Chattering avoidance by second-order sliding mode control. *IEEE Trans. Automat. Contr.* **1998**, *43*, 241–246. [[CrossRef](#)]
22. Amer, A.F.; Sallam, E.A.; Elawady, W.M. Adaptive fuzzy sliding mode control using supervisory fuzzy control for 3 DOF planar robot manipulators. *Appl. Soft Comput.* **2011**, *11*, 4943–4953. [[CrossRef](#)]
23. Xu, G.; Liu, F.; Xiu, C.; Sun, L.; Liu, C. Optimization of hysteretic chaotic neural network based on fuzzy sliding mode control. *Neurocomputing* **2016**, *189*, 72–79. [[CrossRef](#)]
24. Yildiz, Y.; Sabanovic, A.; Abidi, K. Sliding-mode neuro-controller for uncertain systems. *IEEE Trans. Ind. Electron.* **2007**, *54*, 1676–1685. [[CrossRef](#)]
25. Hao, Z.; Xing-Yuan, W.; Xiao-Hui, L. Synchronization of complex-valued neural network with sliding mode control. *J. Franklin Inst.* **2016**, *353*, 345–358. [[CrossRef](#)]
26. Yang, Y.; Yan, Y. Neural network approximation-based nonsingular terminal sliding mode control for trajectory tracking of robotic airships. *Aerosp. Sci. Technol.* **2016**, *54*, 192–197. [[CrossRef](#)]
27. Wu, H.; Wang, L.; Niu, P.; Wang, Y. Global projective synchronization in finite time of nonidentical fractional-order neural networks based on sliding mode control strategy. *Neurocomputing* **2017**, *235*, 264–273. [[CrossRef](#)]
28. Karami-Mollae, A.; Tirandaz, H.; Barambones, O. State tracking control of nonlinear systems using neural adaptive dynamic sliding mode. *Trans. Inst. Meas. Contr.* **2019**, *41*, 3033–3042. [[CrossRef](#)]
29. Boiko, I.; Fridman, L. Analysis of chattering in continuous sliding-mode controllers. *IEEE Trans. Autom. Control* **2005**, *50*, 1442–1446. [[CrossRef](#)]
30. Boiko, I.; Fridman, L.; Iriarte, R. Analysis of chattering in continuous sliding mode control. In Proceedings of the 2005 IEEE American Control Conference (ACC), Portland, OR, USA, 8–10 June 2005; pp. 2439–2444.
31. Man, Z.; Poplinsky, A.P.; Wu, H.R. A robust terminal sliding-mode control scheme for rigid robot manipulators. *IEEE Trans. Autom. Control* **2005**, *39*, 2439–2444.
32. Shao, K.; Zheng, J.; Tang, R.; Li, X.; Man, Z.; Liang, B. Barrier function based adaptive sliding mode control for uncertain systems with input saturation. *IEEE/ASME Trans. Mechatron.* **2022**, *27*, 4258–4268. [[CrossRef](#)]
33. Karami-Mollae, A.; Tirandaz, H. Estimation of load torque in induction motors via dynamic sliding mode control and new nonlinear state observer. *J. Mech. Sci. Tech.* **2018**, *32*, 2283–2288. [[CrossRef](#)]
34. Karami-Mollae, A.; Tirandaz, H.; Barambones, O. Dynamic sliding mode position control of induction motors based load torque compensation using adaptive state observer. *COMPEL* **2018**, *37*, 2249–2262. [[CrossRef](#)]
35. Yousef, H.A.; Wahba, M.A. Adaptive fuzzy MIMO control of induction motors. *Expert Sys. Appl.* **2009**, *13*, 4171–4175. [[CrossRef](#)]
36. Lee, H.; Utkin, V.-I. Chattering suppression methods in sliding mode control systems. *Annu. Rev. Contr.* **2007**, *31*, 179–188. [[CrossRef](#)]
37. Khalid, K.M.; Spurgeon, S.K. Robust MIMO water level control in interconnected twin-tanks using second order sliding mode control. *Contr. Eng. Pract.* **2006**, *14*, 375–386.
38. Laghrouche, S.; Plestan, F.; Glumineau, A. Higher order sliding mode control based on optimal linear quadratic control. In Proceedings of the 2003 European Control Conference (ECC), Cambridge, UK, 1–4 September 2003.
39. Levant, A. Universal SISO sliding-mode controllers with finite time convergence. *IEEE Trans. Automat. Contr.* **2001**, *49*, 1447–1451. [[CrossRef](#)]
40. Levant, A. Higher-order sliding modes, differentiation and output-feedback control. *Int. J. Contr.* **2003**, *76*, 924–941. [[CrossRef](#)]
41. Levant, A. Homogeneity approach to high-order sliding mode design. *Automatica* **2005**, *41*, 823–830. [[CrossRef](#)]
42. Edwards, C.; Spurgeon, S. *Sliding Mode Control: Theory and Applications*; Taylor and Francis: Milton Park, Oxfordshire, 1998.
43. Zhihong, M.; Glumineau, X.H.Y. Terminal sliding mode control of MIMO linear systems. *IEEE Trans. Circuits Syst.* **1997**, *44*, 1065–1070. [[CrossRef](#)]
44. Yang, J.; Li, X.; Fei, J. Intelligent global fast terminal sliding mode control of active power filter. *Mathematics* **2023**, *11*, 919. [[CrossRef](#)]
45. Khalil, H.K. *Nonlinear Systems*; Prentice-Hall: Englewood Cliffs, NJ, USA, 1996.

Disclaimer/Publisher’s Note: The statements, opinions and data contained in all publications are solely those of the individual author(s) and contributor(s) and not of MDPI and/or the editor(s). MDPI and/or the editor(s) disclaim responsibility for any injury to people or property resulting from any ideas, methods, instructions or products referred to in the content.